Investigating the Effect of Explosive Welding Variables on the Corrosion Behavior of Explosive Joint of Two-Layered Inconel 718-AISI H13 Hot Work Tool Steel Plates in Salty Environment

A. Norbakhsh[1], M. R. Khanzadeh GharahShiran[2,*], A. Saadat[2], H. Bakhtiari[3]

[1] Department of Materials Engineering, Bandarabbas Branch, Islamic Azad University, Bandarabbas, Iran.
[2] Center for Advanced Engineering Research, Majlesi Branch, Islamic Azad University, Esfahan, Iran.
[3] Department of Materials Engineering, Najafabad Branch, Islamic Azad University, Najafabad, Iran.

Abstract

In this research, the corrosion behavior and microstructural changes in two-layered Inconel 718- AISI H13 steel plates after the explosive welding process was investigated. The results of polarization curves showed that by comparing the first series of samples (explosive charge 2 and standoff distance of 3 mm), the third series (explosive charge 1 and standoff distance of 3 mm), and the fifth series (explosive charge 3 and standoff distance of 3 mm), it can be found that by increasing the explosive charge and the reduction of concentration at the intersection, the corrosion current density has been reduced. The metallographic results show a wave- vortex-like intersection due to the increased thickness of the explosive charge. The results of hardness testing also showed that when approaching the intersection of joint, the hardness in both samples has been increased. The impedance test resultsfor the welded samples showed that the highest polarization resistance (9407 Ω cm^2) was found for the fifth sample series (explosive charge 3 and standoff distance of 3 mm), followed by the second sample (8341 Ω cm^2) (explosive charge 2 and standoff distance of 4 mm), and the lowest polarization resistance was seen in the third series sample.

Keywords: Explosive Welding, Corrosion, Immersion Test, Polarization Test, Electrochemical Impedance Test

1. Introduction

Explosive welding is one of the solid-state welding processes formed as a result of diagonal collision of two metals at high speeds and under controlled conditions of the joint. In this method, the explosives are used as a source of collision energy creation. Since the collision (which is done diagonally) occurs at very high pressures and in a fraction of a second, it is expected that the two metal surfaces have hydrodynamic behavior in contact with each other [1,2]. The emergence of a flow during welding, under certain circumstances, causes the formation of a plasma jet right in front of the explosion front. This plasma jet causes the superficial atomic layers to detach from the joint position, and a very clean and high quality surface is prepared for welding. Then, as a result of the explosion force, the two oxide- free surfaces are pressed together, and a metallurgical connection is formed as a result of atomic bond formation in the solid state at the intersection [3-6]. The main variables of the method are the number of explosive charges (the ratio of explosives weight to the weight of the flying plate) and the stopping distance. These variables will have a direct impact on metallurgical and mechanical properties of the claddings [3-6].

The collision speed of the plates can be considered as a function of these variables. In this case, by increasing the collision speed, the type of intersection changes from flat to a corrugated one. By following this process, some nodes are formed in the vicinity of the waves, and molten packets or intermetallic compounds may be created at the intersection. Finally, these intermetallic compounds will be distributed as a widespread layer throughout the intersection. Many studies have been conducted on the effects of explosive welding parameters on morphology and properties of the joints concerning various alloys [3-7]. In all of these studies, the overall results have shown that by increasing the amount of explosive charge and the stopping distance, the intersection changes from flat to a corrugated one, and by further increase of these variables, the joint is formed at the intersection as a result of pressure force and the excessive power of intermetallic compounds and even the molten materials [6,7].

Mudali et al [8] investigated the corrosionof titanium explosive joint for 304 stainless steel. Their results showed that the bending test of the joint in the nitric acid medium had acceptable results, and the corrosion attack was mostly concentrated on the intersection of the joint. Also, the aforementioned joint with titanium plate had a good corrosion rate, but the joint fractured in bending test. Rajani et al [9]. Studied the corrosion behavior of explosive joint of Inconel625/ plain carbon steel.

*Corresponding author
Email address: m.khanzadeh@iaumajlesi.ac.ir

Table. 1. The chemical composition of the base and flying plates (wt. %) [14].

Elements	C	Si	Cr	Ni	Mo	Fe	Nb	Mn	V	Ti
AISI H13	0.4200	1.0500	5.0900	0.1200	1.1400	Base	-	0.3500	0.8200	0.0400
Inconel 718	0.0600	0.0200	18.550	Base	3.0200	19.800	4.7500	0.0500	0.0330	0.9500

The results showe that by increasing the explosive charge, the corrosion rate increased, but the corrosion resistance of the metal decreased and this is due to an increase in kinetic energy and the intersection created by increased explosive charge that the increased kinetic energy of collision transferred to the sample along with more explosive charge also affected the increased rate of the corrosion of these samples. Acarer [10] studied the corrosion of aluminum- copper joints made by explosive welding and showed that due to the formation of localized intermetallic compounds at the intersection of the joint, galvanic corrosion occurs. According to their results, the aluminum side of the formed joint is corroded more than the copper layer due to the greater electronegativity. Kahraman et al [11] examined the corrosion behavior of aluminum- titanium bilayer joints. Immersion test showed that weight loss was high at the beginning of immersion test, and over time, the rate of weight loss decreased. Their results also showed that the weight loss in corrosion tests is increased by increasing the deformation caused by the increased explosive charge. Now, given the importance of three-layered explosive joint in industry and the important issue of corrosion in different environments, the impact of the variable of the stopping distance between the plates on the properties of the intersection of three-layered explosive joint made of $AlMg_5$, pure aluminum, and steel is investigated in terms of structural properties, mechanical properties and corrosion, and the optimal stopping distance between the plates will be determined [10,11]. Investigating the effects of the thickness of explosives and the stopping distance on corrosion properties of the intersection of the explosive joint made of Inconel 718- AISI H13 hot work steel using potentiodynamic polarization and electrochemical impedance spectroscopy is a new and novel issue.

2. Materials and Methods
2.1. Materials

Inconel 718 plates in solution annealing conditions and quenched- tempered hot work AISI H13 chromium steel were selected as flying (130 mm × 130 mm × 3.2 mm) and base plates (100 mm × 100 mm × 10 mm), respectively. The chemical composition of plates was determined by emission spectrometry and is given in Table. 1. [12]. After quenching -tempering heat treatments, steel plate was grounded and Inconel plates were mechanically polished.

Before welding, all surfaces of plates were cleaned with acetone solution [12]. The type of explosives was Amatol 95.5 made by combining Trinitrotoluene (5%), and Ammonium Nitrate (95%) at a speed of 2507 meters per second, and an M8 detonator was used. To establish the desired plates to carry out the explosive welding process, a concrete platform covered with a medium of fine sand as an intermediate and buffer layer was considered. Also, in order to create the designed stop distances in each test, copper wires with appropriate diameters to the height of designed stop distances were used between the plates.

To establish the explosives on top of the flying plate, a box made of MDF[1] with appropriate dimensions and a height equivalent to the thickness of the required explosives for the intended test was used and placed inside a wooden box with appropriate dimensions immediately on top of the flying plate. The parallel regulatory arrangement system shown in Fig. 1. was selected for the welding process.

Connecting tests were performed by changing the stopping distance and the explosive charges, and the test conditions given in Table. 2. The explosive charge in the table represents the ratio of weight of the explosives to the weight of the flying plate which is obtained using the following Eq. (1) [12]:

$$(\rho_e * T_e)/(\rho_f * T_f) \qquad \text{Eq. (1)}$$

ρ_e = density of explosives

T_e = thickness of explosives

ρ_f = density of flying plate
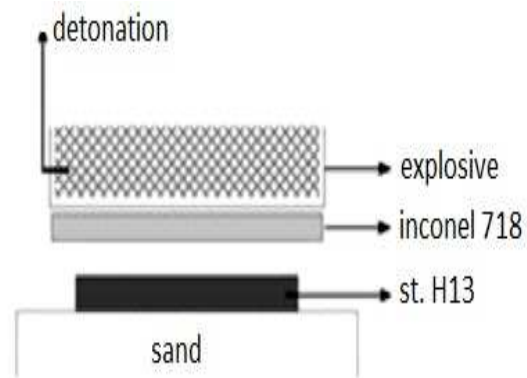
T_f = (thickness of flying plate)

Fig. 1. Parallel arrangement used in the tests.

---

[1]Medium-Density Fiberboard (MDF)

Table. 2. Regulatory characteristics of performed tests and the resulting interfaces.

Test number	Stopping distance(mm)	Explosive charge (R)
1	3	2
2	4	2
3	3	1
4	4	1
5	3	3

2.2. Optical Microscopy Examination

Some samples were prepared with dimensions of 10 mm × 10 mm. First, the samples were cut into small sizes for mounting using a wire-cutter device. The samples were cut perpendicular to the axis of connection and the welding surface and then cold mounted. In order to prepare the samples for metallography, first, the samples surfaces were sanded using sandpaper numbers 60 to 2500.After removing the contours and surface roughness, they were polished by the means of devices, wad and a solution of aluminum oxide. After polishing, the surfaces of the samples were washed and dried with alcohol and then, were etched chemically using Glyceregia solution (glycerol + nitric acid + hydrochloric acid).The reference standards ASTM E 883-11 [13] have been used for optical microscopy imagesand the microstructures of the interface have been analyzed by model Olympusoptical microscope in different magnifications.

2.3. Electrochemical Test

In order to evaluate the corrosion behavior of the parts with explosive welding in a solution of 3.5% NaCl, a three-electrode electrochemical cell with a capacity of 500 mL was used for the polarization and EIS[1] tests. An SCE[2] was used as the reference electrode, and a platinum electrode was used as the auxiliary electrode. All of the electrochemical tests were conducted using EG & G device Model M1025 made in the USA and Pro Power suit 2.20.0 software. Potentiodynamic polarization tests were performed with a scan rate of 1mV/s from the initial potential of -250 mV lower than the open circuit potential to the final potential of 250 mV above the open circuit potential to determine the corrosion current and potential (ASTM G59-97) [14]. EIS test was conducted in the frequency range of 100 KHz to 10 mHz with a range of 10 mV around the open circuit potential using EG & G device Model M1025 made in USA. ZSimpWin 3.22 software was used to analyze the results of EIS. The time required

[1]Electrochemical Impedance Spectroscopy (EIS)

[2] Supersaturated Calomel Electrode (SCE)

to reach the steady state was 90 minutes (ASTM G106) [15].

3. Results and Discussion

Fig. 2. shows the images of waves created in the longitudinal direction of the samples connections.
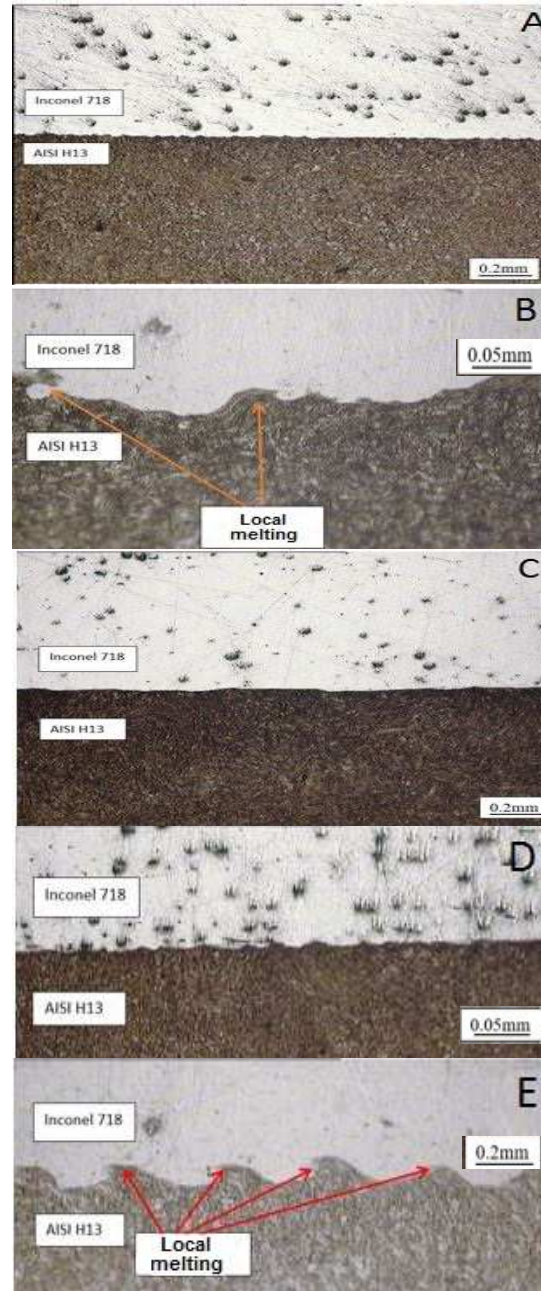

Fig. 2. Optical metallography images of the joint intersection of the samples a) The first series b) The second series c) The third series d) The fourth series e) The fifth series.

As can be seen in Fig. 2(a)., the joint intersection of the first sample in this mode is a short wave. In this case, due to the higher explosive charge compared to that of the third series, it has short waves.Comparing the second series sample with the first series sample with the same explosive charges shows that the stopping distance in the second series sample is longer and therefore, the height and length of waves have been increased due to higher kinetic energy.As shown in Fig. 2(c)., the thickness of the localized molten layer of the joint intersection of third series samples has decreased compared to the first series samples or the same stopping distance (three millimeters). About the shape of intersection as compared to the first series samples (explosive charge 2 and the stopping distance of 3 mm), due to explosive charge reduction and reduction of collisional kinetic energy, the height of waves at the intersection has been decreased and has become as a flattened-wave (Compare Fig. 3. and Fig. 5).In Fig. 2(d)., the intersection of the fourth series sample with the stopping distance of 4 mm and the explosive charge 1 is shown. As can be seen, due to the lower explosive charge, the length and height of waves have been decreased compared to the second series sample and have been increased compared to the third series sample with constant explosive charge and longer stopping distance [16].Fig. 2(e)., shows the intersection of the fifth series sample with the stopping distance of 3 mm and the explosive charge 3. As can be seen, in the fifth series sample as compared to the first and third series samples with the same stopping distance, the explosion charge is higher and as a result, the intersection becomes more corrugated, and the intersection has become wave- vortex- shaped with some localized molten zones.Fig. 3. shows the microscopic images of the melting layer of the samples. For example, the first series in Fig. 3(a)., as shown, is due to the increase in explosive charge and the increase of the kinetic energy of the collision in the interface, the interface is short-wave.Fig. 3(b).,shows scanning electron microscope images of the intersection of the second series samples with a stopping distance of 4 mm and the explosive charge 2.

More corrugation is due to increased stopping distance and increased collisional kinetic energy compared to the first series sample at the intersection. Images of scanning electron microscope of the intersection of the third series sample and formation of localized molten layer is shown in Fig. 3(c). In this sample, the thickness of local molten layer is the lower than the first series.Fig. 4. shows EDS analysis of the localized molten layer shown in Fig. 3(c).
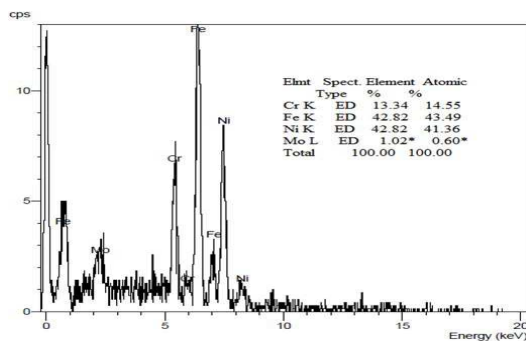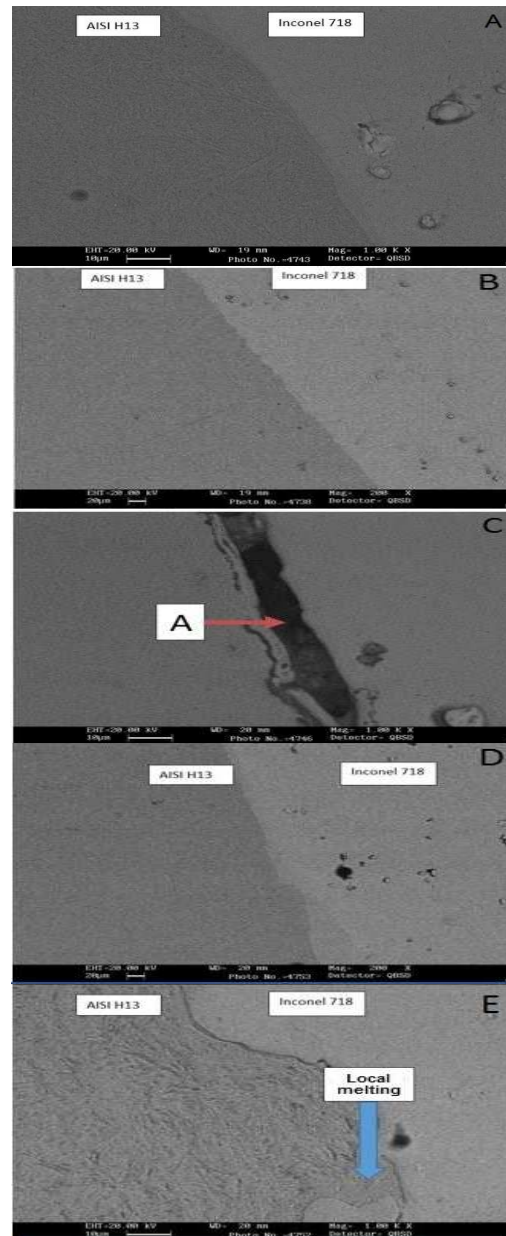

Fig. 3. Scanning electron microscopy images of the locally molten zone at the intersection of the samples: a) The first series b) The second series c) The third series d) The fourth series e) The fifth series.

Fig. 4. EDS analysis of the locally molten zones marked in the third series sample (Fig. 3(C)).

based on which the chemical composition of the local molten layer includes 43.49 atomic percent iron, 14.55 atomic percent Cr, 41.36 atomic percent Ni and 0.6 atomic percent molybdenum. This composition is a mixture of base and flying plates. Fig. 3(d). shows the fourth series sample in which due to the lower explosive charge compared to the second series sample, the thickness of local molten layer is lower.Fig. 3. shows scanning electron microscopy images of the intersection and the localized molten layer of the fifth series sample with a stopping distance of 3 mm and the explosive charge 3. In this case, the greatest thickness of the locally molten layer is observed.Fig. 5. shows the polarization curves of samples of explosive welding.Electrochemical parameters extracted from these curves such as corrosion potential (E_{corr}), corrosion current density (i_{corr}) (corrosion rate), the gradients of anodic and cathodic Tafel obtained using Tafel extrapolation method have been reported in Table. 3. In general, the parallelism of branches of cathodic Tafel in Fig. 5. shows that hydrogen emissions are under the control of activation, and H^+ ions reduction mechanism on samples surfaces is not much affected by welding operations. Anode branches are different in Fig. 5. and influenced by various parametersof explosive welding. No passive layer was observed in the whole samples. The results of Table. 3. showed that by increasing the stopping distance (samples 1 and 2 with explosive charge 2), the corrosion potential decreased from -298 to -342 mV, and corrosion current density increased from 1.73 to 2.08 micro amps per square centimeter.Also an increase can be seen in the stopping distance of samples 3 and 4 (the explosive charge 1) that the corrosion current density has increased from 0.57 to 0.81 micro amps per square centimeter, and this is due to the energy boost in the intersection caused by increased stopping distance that aggravates corrosion [17].To study the effect of explosive charge, we can consider the results of samples 1, 3 and 5 (the stopping distance of 3 mm) and samples 2 and 4 (the stopping distance of 4 mm) that in both cases, by increasing the explosive

charge, the corrosion rate increased and this is due to increased energy of the intersection caused by increased explosive charge.
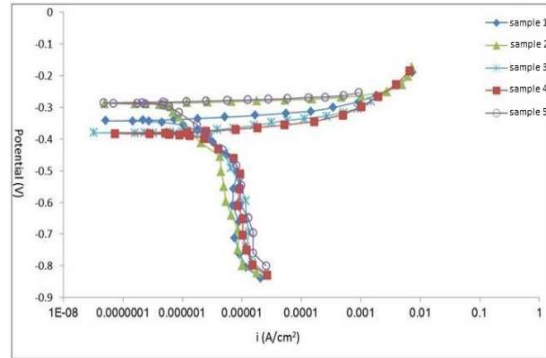

Fig. 5. Potentiodynamic polarization curves of samples of the explosive welding.

The lowest corrosion rate is related to the third sample with 0.57 micro amps per square centimeter and the highest corrosion rate is of the fifth sample with 2.46 micro amps per square centimeter.
The speed of flying plate and dynamic angle of collision are increased by increasing the stopping distance and explosive charge and therefore, the kinetic energy of the collisions is increased. Increased hardness of samples by greater stopping distance reflects the increased amount of kinetic energy of collision transferred to the intersection. Increased energy of this sample has increased the corrosion rate [18].

3.4 Examining the Results of Electrochemical Impedance Spectroscopy

EIS was employed to study the surface layer created by the samples in corrosive environments.
Nyquist diagrams related to explosive welding samples are shown in Fig. 6. EIS data were obtained using the equivalent circuit shown in Fig. 7. which is well-matched with the experimental results and shown in Table. 4.

Table. 3. Electrochemical parameters obtained from potentiodynamic polarization curves obtained using explosive welding in 3.5% NaCl solution at ambient temperature.

Sample	The explosive charge (R)	The stopping distance (mm)	i_{corr} (μAcm^{-2})	E_{corr} (mV)	β_a (mV dec^{-1})	β_c (mV dec^{-1})
1	2	3	1.7300	-289	12.900	109
2	2	4	2.0800	-342	8.5000	248
3	1	3	0.5700	-388	31.700	60.500
4	1	4	0.8100	-386	23	150
5	3	3	2.4600	-286	8.2000	144

Table. 4. EISdata obtained using explosive welding in 3.5% NaCl solution at ambient temperature.

sample	The explosive charge (R)	The stopping distance(mm)	R_s (Ω)	R_p (Ω cm^2)	C_{dl} (μF cm^{-2})	n
1	2	3	14.960	6256	118	0.7600
2	2	4	17.460	5116	142	0.7300
3	1	3	20.640	9407	97	0.8800
4	1	4	11.630	8341	114	0.8000
5	3	3	19.790	4177	157	0.6700

Fig. 6. shows that the impedance loops obtained in Nyquist curve are slightly crushed down as compared to a full half circle, and this phenomenon is known as sagging effect. In general, the deviation from the full half circle is attributed to the frequency dispersion and also, the surface heterogeneities and mass transfer resistance. This difference is described by the non-ideal behavior of the double layer as a capacitor. Therefore, in order to achieve a more accurate conformity in results, due to the distribution of relaxation times caused by available non-uniformities in micro- or nano- surfaces such as roughness, porous layers, impurities, absorption of inhibitors, penetration, etc. it is essential to use a CPE[1] instead of the non-ideal capacitor behavior of double layer. The impedance of a constant phase element is expressed by the following Eq. (2) [18]:

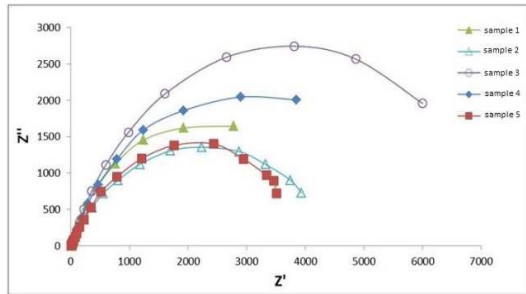$$Z_{CPE} = [Y_0(j\omega)^n]^{-1} \qquad \text{Eq. (2)}$$

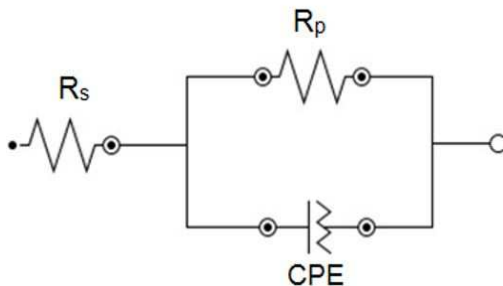**Fig. 6. Nyquist curves of samples of explosive welding.**

Fig. 7. Diagram of equivalent electrical circuit used to model the behavior of metal/solution intersection.

[1]Constant Phase Element (CPE)

Where Y_0 is the relativistic factor (admittance) and n is the non-uniformity coefficient of surface (phase difference), and a greater n means more continuity and uniformity of the welding intersection. In this case, the corrosion current is lower, because the corrosion current is proportional to the contact area of solution with the metal. The more the defects and discontinuities are, the more the efficient contact surface of solution and metal is, and therefore, the corrosion current increases. For n = 0, 1 and 1, CPE shows purely resistive, purely capacitive and purely inductive behaviors, respectively [18].

In this study, the diameter of the Nyquist curves (Fig. 6.) is considered as the polarization resistance (R_P). In other words, the only available capacitive loops are related to charge transfer resistance between the metal and the outer Helmholtz layer. These observations indicate that corrosion of metal is controlled by a charge transfer process.
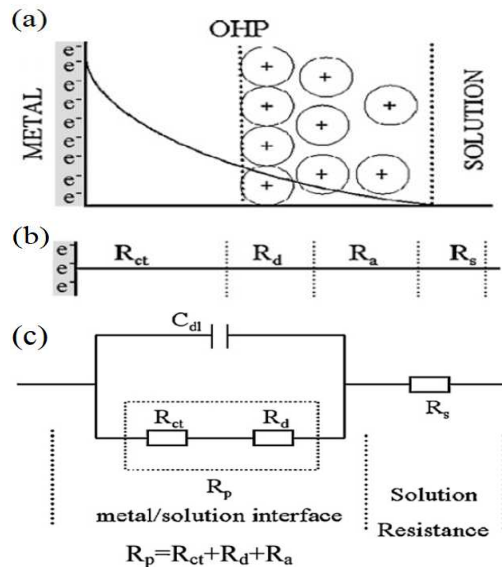

Fig. 8. potential distributions at the metal/solution intersection (a), resistances related to the double layer (b), and equivalent electrical circuit proposed for the solution without inhibitor [18].

Using an equivalent circuit and providing an appropriate model for the metal/solution intersection, electrical double layer can be described well.

Electrical equivalent circuit corresponding to the samples in the solution can be seen in Fig. 8(a). by providing a schematic model for the potential distributions at the metal/solution intersection Fig. 8(b). and resistance related to the double layer Fig. 8(c). In the presence of inhibitors, polarization resistance (R_p), includes charge transfer resistance (R_{ct}), resistance of inhibiting layer on the metal surface (R_f), all the particles (inhibitor molecules, corrosion products, etc.) accumulated at the metal/solution intersection (R_a) and resistance of diffusion layer (R_d) ($R_p = R_{ct} + R_f + R_{a} + R_d$) [18].
Double-layer capacity (C_{dl}) is calculated by the following Eq. (3):

$$f(-Z''_{max}) = \frac{1}{2\pi C_{dl} R_{ct}} \qquad \text{Eq. (3)}$$

Where, $-Z''_{max}$ is the maximum imaginary impedance component.
According to Table. 4., n in sample 1 is greater than sample 2 and thus, the corrosion current is lower in sample 1 which increases charge transfer resistance. Also, in samples 3 and 4, n is greater in the third sample that leads to greater charge transfer resistance. Comparing samples 1, 3 and 5 with the same stopping distance, shows that the explosive charge has changed, and sample 3 by explosive charge 1 has the highest n (0.88), followed by sample 1 with explosive charge 2 ($n = 0.76$), and the lowest n occurs in sample 5 with explosive charge 3 that is due to increased explosive charge and increased kinetic energy at the intersection. Comparison of samples 2 and 4 with identical stopping distances shows that the explosive charge was different, and the higher explosive charge in sample 2 reduces n in this sample that is due to increased kinetic energy and the intersection caused by increased explosive charge. Increased collisional kinetic energy transferred to the sample with higher stopping distance and explosive charges also affect the increased rate of corrosion in these samples. Due to localized molten zones shown in Fig. 3., sample 5 has the lowest n and thus, the least charge transfer resistance [18,19].

4. Conclusions

1. Because of collision of flying plate, the consumed kinetic energy is changed into potential energy, leading to deformation of collisional surfaces.
2. By increasing the stopping distance or the amount of explosive charge due to increased pressure and collision energy and its higher temperature, the quantity of localized molten regions zones at the intersection, especially in the vicinity of wave vortices is increased.
3. According to polarization test, corrosion current density was increased by increasing the stopping distance and the explosive charge.

4. Electrochemical impedance test results show that n in the sample 1 is greater than sample 2 and thus, the corrosion current in sample 1 is lower which increases the charge transfer resistance. Also, in samples 3 and 4, n is higher in the third sample that increases charge transfer resistance.

References

[1] M. Acarer and B. Demir, Mater. Lett., 62(2008), 4158.
[2] F. Fendik, Mater. Des., 32(2011), 1081.
[3] K. Raghukandan, J. Mater. Process. Technol.,139(2003), 573.
[4] S. Jun, T. Jie and G. Zhong, Trans. Nonferrous Met. Soc. China, 21(2011), 2175.
[5] M. Benak, M. Turna, M. Ozvold, P. Nesvadba, J. Lokaj, L. Caplovic, F. Kovac and V. Stoyka,19. Mezinárodní Konference Metalurgie a Material,Sborník Konference Metal, Roznov pod Radhostem Czech Republic, (2010), 235.
[6] S. Saravanan and K. Raghukandan, Mater. Manuf. Processes, 589(2013), 05.
[7] A. Khosravifard and R. Ebrahimi, Mater. Des., 31(2010), 493.
[8] U. Kamachi Mudali, B. M. Ananda Rao, K. Shanmugam, R. Natarajan and B. Raj, J. Nucl Mater., 321(2003), 40.
[9] H. R. Zareie Rajani, S. A. A. Akbari Mousavi and F. Madani Sani, Mater. Des., 43(2013), 467.
[10] M. Acarer, Elec. J. Mater. Eng. Perform., 21(2012), 2375.
[11] N. Kahramana and F. Findik, Int. J. Impact Eng., 34(2007), 1423.
[12] R. hadi, S. A. A. Akbari musavi and H. Ebrahimi, Adv. Mater. Res., 829(2013), 36.
[13] Standard Guide for Reflected-Light Photomicrography, ASTM E88 3-11, Philadelphia, (2014).
[14] Standard Test Method for Conducting Potentiodynamic Polarization Resistance Measurements, ASTM G59 - 97, Philadelphia, (2014).
[15] Standard Practice for Verification of Algorithm and Equipment for Electrochemical Impedance Measurements, ASTM G106 - 89, Philadelphia, (2014).
[16] J. Verma, R. V. Taiwade, J. Manuf. Process., 24(2016), 1.
[17] R. G. de Paula, C. R. Araujo, F. C. Lins, J. R. G. Carneiro, Corros.Eng. Sci. Techn., 47(2012), 116.
[18] K. Srinivasa and K. Rao Prasad Rao, Trans. Indian Inst. Met., 57(2004), 593.
[19] H. Liqing, L. Guobiao, W. Zidong, Z. Hong, L. Feng and Y. Long, Rare. Metal Mat. Eng., 39(2010), 393.